

Guava® and Amnis®  
Flow Cytometers  
are Now Part of Luminex.



**Luminex**  
complexity simplified.



## Antibody Binding to Individual Short Consensus Repeats of Decay-Accelerating Factor Enhances Enterovirus Cell Attachment and Infectivity

This information is current as of March 22, 2019.

Darren R. Shafren, Douglas J. Dorahy, Rick F. Thorne, Taroh Kinoshita, Richard D. Barry and Gordon F. Burns

*J Immunol* 1998; 160:2318-2323; ;  
<http://www.jimmunol.org/content/160/5/2318>

**References** This article **cites 25 articles**, 17 of which you can access for free at:  
<http://www.jimmunol.org/content/160/5/2318.full#ref-list-1>

**Why *The JI*?** [Submit online.](#)

- **Rapid Reviews! 30 days\*** from submission to initial decision
- **No Triage!** Every submission reviewed by practicing scientists
- **Fast Publication!** 4 weeks from acceptance to publication

*\*average*

**Subscription** Information about subscribing to *The Journal of Immunology* is online at:  
<http://jimmunol.org/subscription>

**Permissions** Submit copyright permission requests at:  
<http://www.aai.org/About/Publications/JI/copyright.html>

**Email Alerts** Receive free email-alerts when new articles cite this article. Sign up at:  
<http://jimmunol.org/alerts>



# Antibody Binding to Individual Short Consensus Repeats of Decay-Accelerating Factor Enhances Enterovirus Cell Attachment and Infectivity<sup>1</sup>

Darren R. Shafren,<sup>2\*</sup> Douglas J. Dorahy,<sup>†</sup> Rick F. Thorne,<sup>†</sup> Taroh Kinoshita,<sup>‡</sup> Richard D. Barry,<sup>\*</sup> and Gordon F. Burns<sup>†</sup>

Decay-accelerating factor (DAF), a widely expressed membrane complement-regulatory protein, is utilized as a cellular receptor by many human enteric pathogens. We show here that the binding of two enteroviruses to individual short consensus repeats (SCR) of DAF on the cell surface is greatly augmented by mAb binding to an alternate SCR: Coxsackievirus A21 binding to the SCR1 of DAF is increased by Ab binding to SCR3 and, conversely, Echovirus 7 binding to SCR3 is enhanced severalfold by Ab binding to SCR1. These Ab-induced increases in viral binding also resulted in increased viral infectivity. Using purified soluble DAF in a solid phase assay it was found that Ab binding to SCR1 is increased greatly in the presence of an Ab against SCR3 and, reciprocally, Ab against SCR1 greatly increases Ab binding to SCR3. In contrast to the results obtained with the larger viral particles, however, this reciprocal Ab-induced enhancement of binding is not seen when measuring Ab binding to membrane-bound DAF SCR on the cell surface. These findings provide a possible explanation for functional differences between membrane-bound and soluble DAF with implications for a potential role for DAF-binding molecules in regulating DAF function. This is the first demonstration of enhancement of viral infectivity mediated by Ab against the viral receptor. *The Journal of Immunology*, 1998, 160: 2318–2323.

**D**ecay-accelerating factor (DAF)<sup>3</sup> is a 70-kDa glycoposphatidylinositol-anchored glycoprotein that protects autologous cells from attack by complement proteins (1). The DAF molecule from the N terminus consists of four short consensus repeats (SCR), a Ser/Thr-rich region containing O-linked glycosylation sites, and a membrane anchoring unit (1, 2). DAF expression is almost ubiquitous throughout the human body, present on the surface of cells in contact with serum (3–6). Ab mapping studies have revealed that only Abs directed against DAF SCR3 totally block the complement regulatory functions of DAF (7). SCR deletion studies have indicated that removal of SCR1 has no effect on DAF function, while deletion of SCR2, SCR3, or SCR4 abolishes DAF function (7).

DAF protects cells from complement-mediated lysis by blocking the C3 and C5 convertases of the classical and alternate pathways (1). DAF prevents formation of cleavage fragments C3a and C5a and furthermore inhibits the amplification of the C cascade on the surface of host cells. Purified soluble DAF can inhibit complement activation in vitro and in vivo (8). However, the anticomplement activity of purified DAF is substantially increased when it

is reincorporated in the cell membrane (8, 9), suggesting that membrane anchoring of DAF induces favorable changes in its functional conformation.

Recently, DAF has additionally been shown to interact with a number of cell surface molecules, and also with human intestinal pathogens. DAF has been proposed as a cellular ligand of CD97 (10), an activation-induced Ag on leukocytes, and has been shown to share a spatial association with coexpressed intercellular adhesion molecule-1 (11). *Escherichia coli*-bearing adhesins of the Dr family bind to DAF SCR3 (12), and an increasing number of human enteroviruses are being shown to bind to different DAF epitopes. Coxsackievirus A21 binds to DAF SCR1 (11), while Coxsackievirus B3 and a number of echoviruses bind to epitopes located in DAF SCR2 and SCR3 (13–16). However, the role of DAF other than as an initial attachment receptor in the infection mechanism of these pathogens is unclear and is currently an area of much investigation. Interestingly, many of these viruses can infect the cells of many human tissues that have been reported to be surrounded by fluids containing soluble forms of DAF (17).

In this report we investigated whether a potential cause for the reduced antienteroviral activity of purified soluble DAF compared with the membrane-bound DAF was due to a reduced accessibility to the functional third SCR. Competitive Ab binding studies revealed that Ab binding to DAF SCRs 1 and 3 of purified non-membrane-bound DAF can be substantially increased by prior exposure to mAbs against SCRs 3 and 1, respectively. An unexpected finding of this study was that pretreatment of membrane-bound DAF with mAbs to SCRs 1 and 3 dramatically enhanced the respective cellular attachment and infectivity of the human enteroviruses echovirus 7 (E7), which binds SCR3, and Coxsackievirus A21 (CAV21), which binds SCR1. This finding is the first report of an antiviral receptor Ab enhancement of viral infectivity that does not involve Fc-receptor interactions.

\*Department of Microbiology and <sup>†</sup>Cancer Research Unit, Faculty of Medicine, The University of Newcastle, Newcastle, New South Wales, Australia; and <sup>‡</sup>Department of Immunoregulation, Research Institute of Microbial Diseases, Osaka University, Suita, Osaka, Japan

Received for publication June 23, 1997. Accepted for publication November 5, 1997.

The costs of publication of this article were defrayed in part by the payment of page charges. This article must therefore be hereby marked *advertisement* in accordance with 18 U.S.C. Section 1734 solely to indicate this fact.

<sup>1</sup> This research was supported by a project grant from the National Health and Medical Research Council of Australia.

<sup>2</sup> Address correspondence and reprint requests to Dr. Darren Shafren, Department of Microbiology, Faculty of Medicine, The University of Newcastle, Newcastle, New South Wales 2300, Australia. E-mail address: dshafren@mail.newcastle.edu.au

<sup>3</sup> Abbreviations used in this paper: DAF, decay-accelerating factor; SCR, short consensus repeats; RD, rhabdomyosarcoma; FcR, Fc receptor.

## Materials and Methods

### Cells, viruses, and Abs

CHO-DAF cells were obtained from Dr. Douglas Lublin, Department of Pathology, Washington School of Medicine, St. Louis, MO (7). HeLa-B cells, rhabdomyosarcoma (RD) cells, echovirus 7 (Wallace), and Coxsackievirus A21 (Kuy Kendall) were obtained from Dr. Margery Kennett, Enteropulmonary Laboratory, Fairfield Hospital, Melbourne, Australia. Anti-DAF mAbs IA10 (IgG2a), VIIIA7 (IgG1), and IH6 (IgG1) were prepared as described (18); mAb IH4 (IgG1) (7) was supplied by Dr. Bruce Loveland, Austin Research Institute, Heidelberg, Australia, and mAb IC6 (19) was supplied by Dr. T. Fujita, Department of Biochemistry, Fukushima Medical College, Fukushima, Japan. The anti PTA-1 mAb (A1; IgG1) was supplied by Dr. G. F. Burns and prepared as described (20). mAb CLB-CD97L1 (IgG1) (10) was supplied by Dr. J. Hamann, Central Laboratory of the Netherlands Red Cross Blood Transfusion service, University of Amsterdam, Amsterdam, The Netherlands. All mAbs used in this study were purified from ascites fluids.

### $F(ab')_2$ preparation

$F(ab')_2$  Ab fragments were prepared from whole mAb VIIIA7 (IgG1) by digestion with resin immobilized-*ficin* and protein G gel chromatography according to the manufacturer's protocol (Immunopure Kit no. 44880; Pierce, Rockford, IL).

### Virus binding assays

CHO-DAF or RD cell monolayers in 24-well tissue culture plates were first incubated for 1 h at 22°C with mAbs A1, IA10, VIIIA7, IH4, and IH6 (20  $\mu$ g/ml) in DMEM containing 1% BSA (DMEM-BSA) and then washed and incubated with purified  $^{35}$ S-labeled CAV21 or E7 ( $4 \times 10^5$  cpm) for the same period. Following four washes with PBS, the cell monolayers were dissolved in 200  $\mu$ l of 0.2 M NaOH-1% SDS and the amount of labeled virus that was bound was measured by liquid scintillation counting. Results are expressed as the means of triplicate wells + SD.

### Virus infectivity assays

RD cell monolayers in 96-well plates were incubated with 50  $\mu$ l of a control mAb and mAbs to each DAF SCR (20  $\mu$ g/ml) diluted in DMEM for 1 h at 37°C. Cells were then challenged with 10 to  $10^4$  50% tissue culture infectious doses (TCID<sub>50</sub>)/well of either E7 or CAV21 in DMEM containing 1.0% FCS (DMEM-FCS) and incubated at 37°C for 48 h. To quantitate cell survival, monolayers were incubated with a crystal violet/methanol solution, washed with distilled H<sub>2</sub>O, and the plates were read on a multiscan ELISA plate reader (Flow Laboratories, McLean, VA) at a wavelength of 540 nm. Results are expressed as mean percentage cell lysis relative to uninfected cell monolayers.

### DAF ELISA

Wells of a microtiter plate were coated with 100  $\mu$ l of mAb IH6 (4.5  $\mu$ g/ml) for 4 h at 37°C, washed, and incubated with 100  $\mu$ l of either purified DAF (0.5  $\mu$ g/ml) or supernatant from DAF-expressing HeLa-B cells incubated with phosphatidylinositol-specific phospholipase C (1.0 U/10<sup>6</sup> cells) for 1 h at 37°C. The purified DAF was supplied by Dr. Tomita, Showa University, Showa, Japan (21). The plate was washed three times with PBS containing 0.05% Tween-20 (PBS-Tween) and incubated with 0.1 ml of anti-DAF mAbs (10  $\mu$ g/ml) for 1 h at 37°C. The plate was washed as before and incubated with 100  $\mu$ l of biotinylated-IH4 (1  $\mu$ g/ml) for 30 min at 37°C. Following three washes with PBS-Tween, 0.1 ml of a 1:1000 dilution of avidin-horseradish peroxidase conjugate (Amersham Life Science, Amersham, U.K.) was added to each well and the plate was incubated for 30 min at 37°C. The plate was washed three times more, 100  $\mu$ l of tetramethylbenzidine solution was added to each well, and the plate was incubated for 15 min at 37°C. The reaction was stopped by the addition of 100  $\mu$ l of 2 M H<sub>2</sub>SO<sub>4</sub>, and the absorbance was measured at 450 nm.

### Flow cytometry

RD cells ( $5 \times 10^5$ ) were incubated with the appropriate mAbs (10  $\mu$ g/ml) diluted in PBS containing 1% BSA (PBS-BSA) at 0°C for 30 min, after which the cells were washed with 5.0 ml of PBS-BSA. The cells were then pelleted at 1000  $\times g$  for 5 min and resuspended in 100  $\mu$ l of fluorescein isothiocyanate-conjugated goat anti-mouse Ig G (heavy plus light chains) (Silenus, Melbourne, Australia) diluted in PBS-BSA. Following incubation at 0°C for 30 min, the cells were washed and pelleted as above, resuspended in PBS-BSA, and analyzed with a FACStar analyzer (Becton Dickinson, Sydney, Australia). For the competitive anti-DAF mAb binding assays, RD or CHO-DAF cells ( $5 \times 10^5$ ) were preincubated with the

Table I. Flow cytometric analysis of the relative binding of different anti-DAF mAbs to the surface of RD cells

Anti-DAF mAbs <sup>a</sup>	Mean Peak Shift $\pm$ SD
No MAB	5.05 $\pm$ 0.35
Control	6.18 $\pm$ 0.64
SCR1 <sup>b</sup>	243.97 $\pm$ 13.0
*SCR1	48.93 $\pm$ 1.37
SCR2	30.53 $\pm$ 1.27
SCR3	61.36 $\pm$ 6.39
*SCR3	40.12 $\pm$ 1.32
SCR4	42.28 $\pm$ 1.91

<sup>a</sup> 10  $\mu$ g/ml.

<sup>b</sup> Control mAb (PTA-1), SCR1 (IA10), \*SCR1 (CLB-CD97L1), SCR2 (VIIIA7), SCR3 (IH4), \*SCR3 (IC6), SCR4 (IHH6).

appropriate anti-DAF mAbs (10  $\mu$ g/ml) for 30 min at 0°C, washed with PBS, then exposed to biotinylated mAbs IA10 or IH4 (1  $\mu$ g/ml) for a further 30 min at 0°C. Cells were then washed with PBS and incubated with phycoerythrin-conjugated streptavidin (Sigma Chemical Co., St. Louis, MO) for 30 min at 0°C, washed with PBS, and analyzed as above.

## Results

### Ab accessibility to membrane-bound and soluble DAF

Competitive mAb binding was used to examine the accessibility of mAbs directed against individual SCRs of both membrane-bound and soluble DAF. We used biotinylated mAbs IA10 and IH4 against DAF SCR1 (a nonfunctional SCR) and DAF SCR3 (a functional SCR), respectively, as our detecting Abs. Ab blockade by mAb IA10 does not block DAF function, while mAb IH4 totally abolishes DAF (7). Flow cytometric analysis revealed similar levels of binding of all anti-DAF mAbs to the surface of RD cells, except mAb IA10 (SCR1), which bound to a significantly higher level (Table I). Subsequent flow cytometric studies revealed a considerable degree of binding of mAb IA10 (10  $\mu$ g/ml) to the surface of non-DAF-transfected COS and CHO cells (e.g., mean intensity fluorescence of mAb IA10 and mAb IH4 binding to mock-transfected COS cells of 125.02 and 7.51, respectively; mean intensity fluorescence of mAb IA10 and mAb IH4 binding to DAF-transfected COS cells of 303.1 and 199.56, respectively). This Ab also did not immunoprecipitate DAF-specific proteins from biotinylated COS cells (11) and did not show increased binding to purified DAF (Fig. 2). Therefore, nonspecific binding seen in RD cells may account for the increased binding levels of this mAb compared with other anti-DAF mAbs observed in this study. The binding of biotinylated anti-DAF mAbs to membrane-bound DAF on the surface of RD cells was quantitated by flow cytometry. RD cells ( $5 \times 10^5$ ) were preincubated with the panel of anti-DAF mAbs (10  $\mu$ g/ml) before incubation with either biotinylated IA10 or IH4 (5  $\mu$ g/ml) and phycoerythrin-conjugated streptavidin. The data in Figure 1A indicate that the binding of mAb IA10 was not significantly affected by the prior binding of any of the panel of mAbs excluding mAb CLB-L1 (SCR1) and itself, while the binding of IH4 was only totally blocked by mAb IC6 (SCR3) and itself (Fig. 1B). The capacity of VIIIA7 to partially block IH4 binding may be explained by the finding that its attachment to SCR2 is influenced by epitopes located in SCR3 (7). The slight inhibitory effect on mAb IH4 binding exerted by mAb IA10 may be due to nonspecific steric hindrance created as a result of its increased binding to RD cells relative to the other anti-DAF mAbs (Table I) when used at a concentration of 10  $\mu$ g/ml. Similar results were obtained when CHO cells stably expressing human DAF (7) were employed (data not shown).

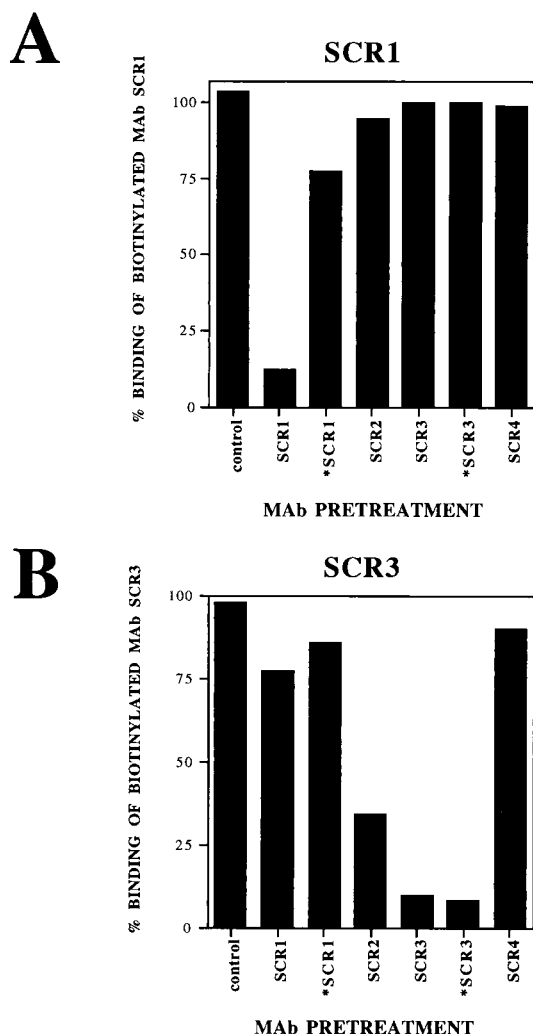


**FIGURE 1.** Suspensions of RD cells ( $5 \times 10^5$ ) were preincubated with a control mAb (A1) or anti-DAF mAbs IA10 (SCR1), CLB-CD97L/1 (SCR1\*), VIIIA7 (SCR2), 1C6 (SCR3\*), IH4 (SCR3), and I1H6 (SCR4) before the addition of biotinylated mAbs IA10 or IH4 and phycoerythrin-conjugated streptavidin. Levels of biotinylated mAb IA10 and mAb IH4 binding were determined by flow cytometric analysis as described in *Materials and Methods*. Percent binding = mean peak shift of biotinylated mAb after mAb pretreatment/mean peak shift of biotinylated mAb with no mAb pretreatment  $\times 100$ .

To assess mAb binding to soluble DAF, purified soluble DAF (21) was immobilized onto a solid phase by capture with an anti-DAF SCR4 mAb. The immobilized DAF was then incubated with the same panel of anti-DAF mAbs as above and spatial changes, if any, in DAF structure were detected by monitoring subsequent binding levels of biotinylated-anti-DAF SCR1 and SCR3 mAbs. The data in Figure 2A show that in this environment, preincubation with mAbs to DAF SCRs 2 and 3 significantly increased the binding of mAb IA10. Conversely, preincubation with the anti-DAF SCR1 mAbs IA10 and CLB-CD97L/1 significantly increased the binding of the anti-DAF SCR3 mAb IH4 (Fig. 2B). In contrast to the binding data to membrane-bound DAF (Fig. 1B), mAb VIIIA7 slightly increased and mAb 1C6 failed to completely block IH4 binding (Fig. 2B). An almost identical pattern of results was observed when DAF cleaved from the surface of HeLa cells by phosphatidylinositol-specific phospholipase treatment was captured onto the solid phase (data not shown). As the purified soluble

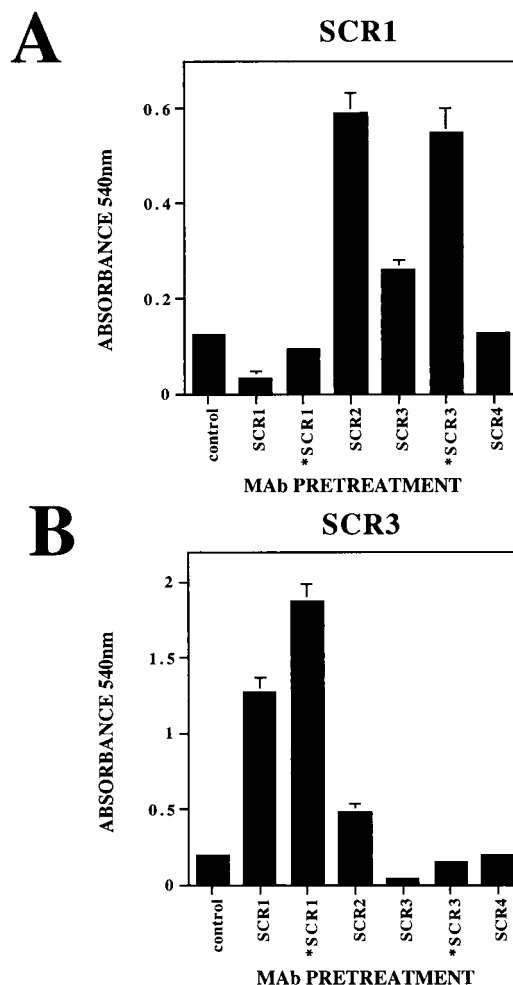


**FIGURE 2.** Binding of biotinylated anti-DAF mAbs to solid phase immobilized DAF. A, Purified DAF ( $0.5 \mu\text{g/ml}$ ) was captured on a solid phase by an anti-DAF mAb I1H6 (SCR4). The immobilized DAF was preincubated with a control mAb (A1) or anti-DAF mAbs IA10 (SCR1), CLB-CD97L/1 (SCR1\*), VIIIA7 (SCR2), 1C6 (SCR3\*), IH4 (SCR3), and I1H6 (SCR4) before the addition of biotinylated mAbs IA10 or IH4. Levels of DAF-bound biotinylated mAb IA10 and mAb IH4 were determined using the ELISA procedure described in *Materials and Methods*. Results are expressed as the mean absorbance (540 nm) of triplicate wells + SD and are representative of two independent experiments.

DAF used in this experiment was immobilized to the solid phase by Ab capture (anti-SCR4), a possible indirect effect exerted by this mAb either alone or in combination with the pre-treating mAb on binding of the appropriate biotinylated mAb cannot be disregarded.

#### *Ab binding to membrane-bound DAF enhances Coxsackievirus A21 (CAV21) and Echovirus 7 (E7) cell binding and lytic infection*

Next we investigated whether anti-DAF mAb binding to surface-expressed DAF could influence the attachment of other DAF-binding ligands such as the human enteroviruses, CAV21 and E7. Echovirus 7 binds to DAF SCR3 (16, 22), and we have recently shown that CAV21 binds to DAF SCR1 (11). However, despite expressing DAF on their cell surfaces, RD (a cell line commonly used for the primary isolation of human enteroviruses) and CHO-DAF cells bind relatively low levels of radiolabeled CAV21 and E7, a finding that may account for their lack of viral susceptibility.



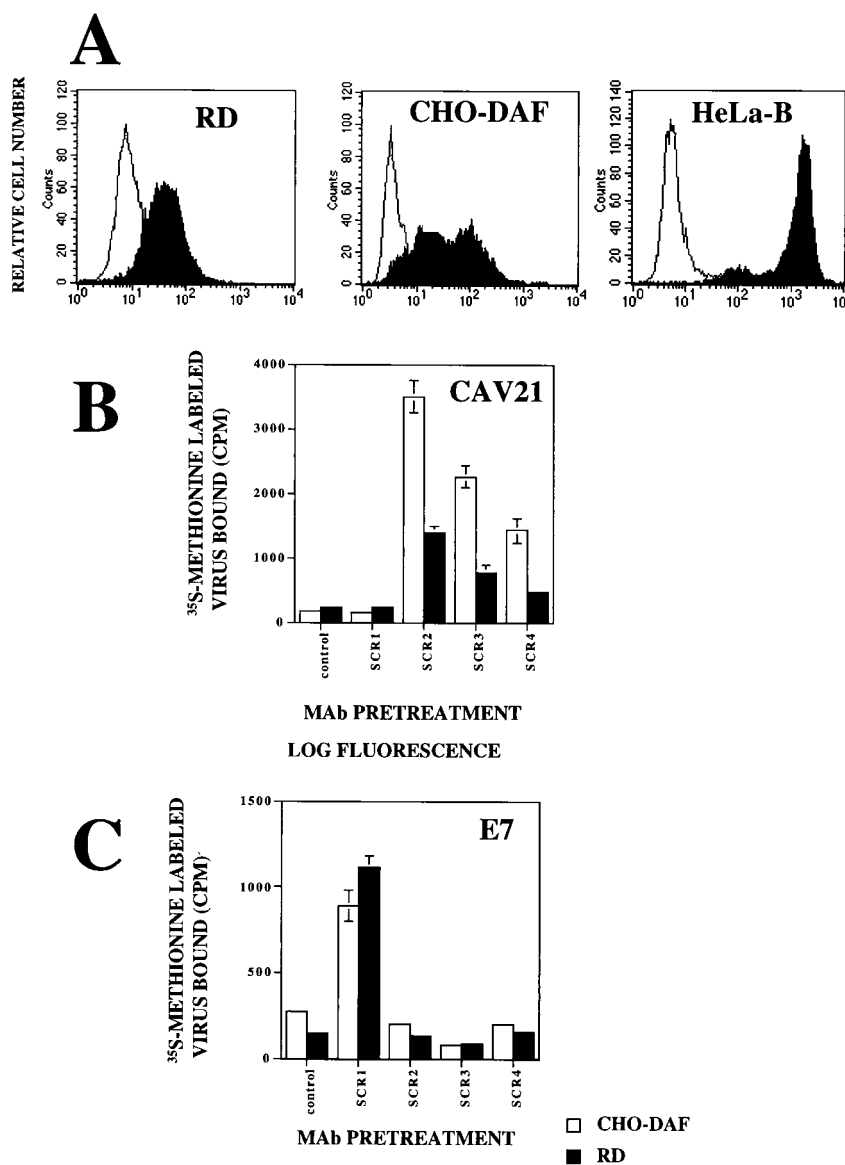


**FIGURE 3.** Anti-DAF mAb-induced enterovirus binding to RD and CHO-DAF cells. *A*, Flow cytometric analysis of DAF expression on the surface of RD, CHO-DAF, and HeLa-B cells. The open histograms represent the binding of the phycoerythrin-conjugated streptavidin, while the closed histograms represent the binding of biotinylated anti-DAF SCR3 (IH4) mAb. Confluent monolayers of RD and CHO-DAF cells in 24-well tissue culture plates were incubated with anti-DAF mAbs IA10 (SCR1), VIIIA7 (SCR2), IH4 (SCR3), IIH6 (SCR4), or control mAb (A1) before addition of purified [<sup>35</sup>S]methionine-labeled (AV21 (*B*) or E7 (*C*)). Results are expressed as the mean of triplicate wells  $\pm$  SD.

To determine whether the low level of CAV21 and E7 binding was a direct result of low DAF surface expression, flow cytometric analysis was used to assess the relative levels of DAF expression on the surface of RD and CHO-DAF to that of the highly permissive HeLa-B cell line (Fig. 3*A*). The fluorescence histograms indicate that the permissive HeLa-B cells expressed significantly higher levels of DAF than either RD or CHO-DAF cells.

Next we assessed the effect of anti-DAF mAb pretreatment on enteroviral binding to RD and CHO-DAF cells. In the case of CAV21, the anti-DAF SCR1 mAb surprisingly had little effect on reducing binding to either RD or CHO-DAF cells (Fig. 3*B*). However, mAbs recognizing DAF SCR2, 3, and 4 increased CAV21 binding by between 6- to 15-fold on CHO-DAF cells and 3- to 7-fold on RD cells (Fig. 3*B*). As expected for specific binding to DAF, anti-DAF SCR3 mAb reduced the binding of E7 to both RD and CHO-DAF cells. However, preincubation of both RD and CHO-DAF cells with an anti-DAF SCR1 mAb increased E7 binding by approximately 5-fold, while mAbs directed against DAF SCR2 and 4 had minimal effect on binding (Fig. 3*C*). These results paralleled the enhanced Ab binding of the biotinylated anti-DAF mAbs to SCR1 and SCR3 to solid phase immobilized DAF

preincubated with mAbs to DAF SCR3 and SCR1, respectively (Fig. 2).

The next step in the investigation was to determine whether Ab-induced enhancement of viral binding increased the susceptibility of RD cells to lytic infection by either E7 or CAV21. Confluent monolayers RD cells in 96-well microtiter plates were preincubated with each of the anti-DAF mAbs and challenged with CAV21 or E7. Viral infection was allowed to proceed for 2 days at 37°C. The cell monolayers were then assayed for cell survival. The data (Fig. 4*A*) indicated that RD cells were rendered highly susceptible to CAV21 lytic infection by pretreatment with the anti-DAF SCR2 and SCR3 mAbs. Conversely, E7-induced cell lysis of the RD cells was increased dramatically following monolayer pretreatment with a mAb to DAF SCR1 (Fig. 4*A*). The enhancement of E7 and CAV21 infectivity by the anti-DAF SCR1 and SCR3 mAbs, respectively, was shown to occur in a dose-dependent manner (Fig. 4*B*). Pretreatment of RD cells with the anti-SCR1 mAb at a concentration as low as 10 ng/ml significantly increased cell susceptibility to E7-induced lytic infection, while CAV21-mediated RD cell lysis was enhanced by an anti-SCR3 mAb, limiting at a concentration of 100 ng/ml (Fig. 4*B*).

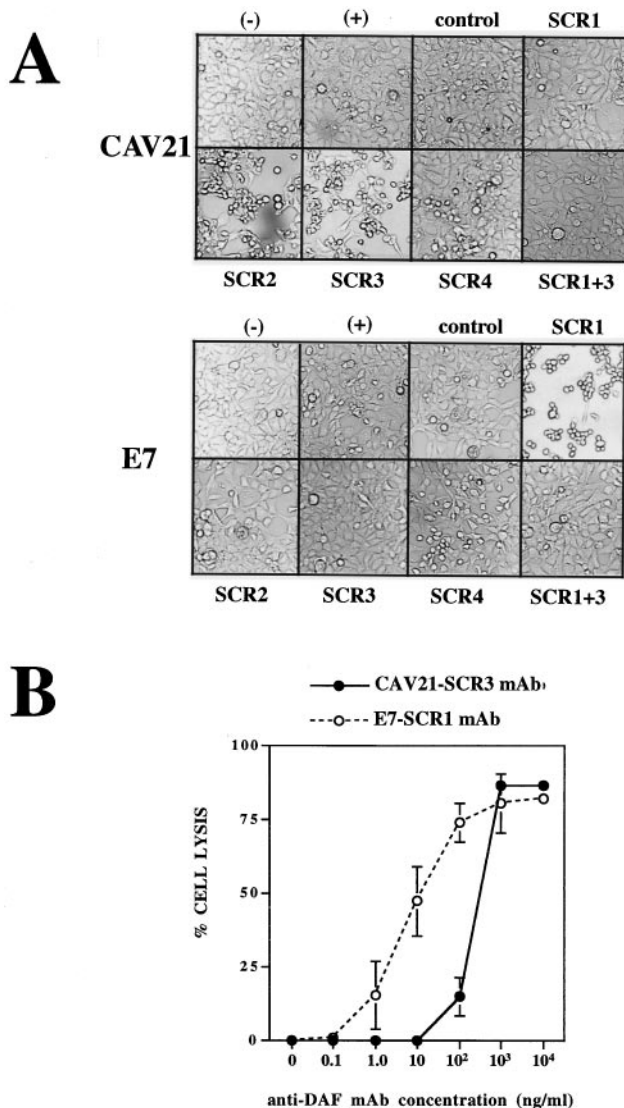


**FIGURE 4.** Anti-DAF mAb-induced enterovirus lysis of RD cells. *A*, Confluent monolayers of RD cells in 96-well culture plates were preincubated with a control mAb (A1), or anti-DAF mAbs IA10 (SCR1), VIIIA7 (SCR2), IH4 (SCR3), and IHH6 (SCR4) before challenge with CAV21 or E7. Following incubation for 48 h at 37°C, cell monolayers were examined for signs of cell lysis and then photographed at a magnification of  $\times 20$  with Kodak Technical Pan 100 ASA film. (–) represents uninoculated RD cells; (+) represents virus-inoculated RD cells. *B*, Titration of anti-DAF mAb-induced CAV21 and E7-mediated cell lysis. RD cell monolayers were preincubated with 10-fold dilutions of anti-DAF SCR1 mAbs IA10 or SCR3 mAb IH4 before challenge with E7 and CAV21, respectively. Following incubation for 48 h at 37°C, cell lysis was assessed by staining the monolayers with a crystal violet solution, and then measuring the absorbance at 540 nm. Results are expressed as the mean % cell lysis of triplicate wells  $\pm$  SD.

*Ab-enhanced enterovirus binding and lytic infection are not mediated by Fc receptors (FcRs)*

It was important to establish that enhancement of viral binding and infectivity induced by the anti-DAF mAbs was the direct result of changes to the receptor itself, and was not caused by a phenomenon analogous to antiviral Ab-dependent enhancement of viral infectivity (23). Ab-dependent enhancement of viral infectivity occurs independent of the virus-cell receptor interaction and has been shown to increase the susceptibility of many cells to viral infection

(e.g., HIV (23), dengue virus (24), foot and mouth disease virus (25)). In this phenomenon, cell infectivity is increased when non-neutralizing antiviral Ab binds to the virus and the complex is in turn bound by the FcR of the target cell, independent of its natural viral attachment receptor.

This was shown to be the case by four parameters: 1) CHO cells lack FcRs (25) and by indirect immunofluorescence analyzed by flow cytometry we were unable to identify any FcRs on the RD cells (data not shown); 2) a blocking mAb to FcR2 had no effect on CAV21 infectivity of RD cells and, in particular, did not influence the enhancement of infectivity induced by the anti-DAF SCR3 mAb (data not shown); 3) F(ab')<sub>2</sub> fragments of mAb VIIIA7 enhanced comparable levels of CAV21 cell lysis to that induced by whole mAbs VIIIA7 and IH4 (data not shown); 4) the increased infectivity and lysis of E7 on RD cells treated with anti-DAF SCR1 mAb was completely inhibited by cotreatment of the cells with anti-DAF SCR3 mAb, which blocks specific viral attachment to this receptor (Fig. 4B). Conversely, the enhanced infectivity of CAV21 induced by the anti-DAF SCR3 mAb was abolished by the coincubation with the anti-DAF SCR1 mAb that blocks binding of this virus to DAF (Fig. 4B).

## Discussion

The data presented here show that Ab binding to individual SCRs of membrane-bound DAF have a dramatic effect on enterovirus binding and consequent infectivity. Preincubation of DAF-expressing cells with mAbs directed against different DAF SCRs significantly enhanced either CAV21 or E7 cell binding but not that of anti-DAF mAbs that bind to similar epitopes. As the CAV21 and E7 particle size ( $\sim 20$ – $25$  nm) is significantly greater than of an Ab molecule binding region, we suggest that these viruses were able to test more rigorously the spatial accessibility of different DAF epitopes. It is possible that cleavage of the glycoposphatidylinositol linkage of membrane-bound DAF and its subsequent attachment to a solid phase induces further rearrangement such that SCR3 (or at least the epitope bound by mAb IH4) becomes cryptic. Consequently, in the solid phase assay the postulated cryptic epitope was exposed by treatment of the bound DAF with a mAb to SCR1 of DAF, and this indicates that an Ab-mediated change may expose the virus and Ab binding site on SCR3. This apparent increased accessibility to the functional third DAF SCR following Ab interactions with the nonfunctional SCR1 suggests a reduced spatial accessibility to DAF SCR3 of purified soluble DAF compared with membrane-bound DAF. Soluble DAF, such as that found in plasma and urine (17), may also be in a configuration similar to that analyzed in the solid phase. If this can be shown to be the case, our findings carry considerable implications toward understanding the reported functional differences between soluble and membrane-bound DAF (8, 9). In this regard, we have found that DAF on the surface of untreated RD cells permits a degree of E7 binding and cell entry (Figs. 3 and 4), whereas in preliminary studies we have been totally unable to inhibit cell infection by E7 with soluble DAF (data not shown).

The findings generated from this study not only provide insights into DAF structure but also impact in the area of clinical diagnostic virology. Their potential advantages are in the forms of 1) increased sensitivity for enterovirus-induced cytopathology testing and 2) an alternate approach to primary virus identification by monitoring differences in viral growth rates following antireceptor Ab-mediated changes in receptor structure.

The data presented here were obtained using an in vitro model; could this phenomenon occur in vivo? The prospect of anti-DAF Ab inducing changes in DAF structure within the body is unlikely.

More probable is the ability of DAF-ligand interactions to enhance enterovirus binding. Thus, interactions between CD97, recently identified as a ligand for DAF or intercellular adhesion molecule-1 and membrane-bound DAF may facilitate enhanced usage of DAF as a functional enterovirus receptor. The exact CD97 binding domain on DAF has as yet not been identified, but preliminary evidence indicates that there may be multiple binding epitopes (10). It can also be speculated that binding of many enteric pathogens to DAF may have a direct regulatory effect on DAF receptor usage. For example, binding of *E. coli*-bearing adhesins of the Dr family to DAF SCR3 (13) may be sufficient to modulate DAF usage by a SCR1 binding virus such as CAV21 (11). Interestingly, in preliminary investigations, preincubation of CHO-DAF cells with either unlabeled CAV21 or E7 facilitated an increased level of binding of radiolabeled E7 and CAV21, respectively. Whether such Ab-mediated enhancement of enterovirus binding to DAF occurs by a mechanism similar to that reported for activating anti-integrin Abs (26) awaits further study.

## Acknowledgments

We gratefully acknowledge those investigators mentioned in the text for the provision of mAbs and purified reagents that enabled this study to be undertaken. We also thank Dr. Douglas Lublin for the critical review of the manuscript.

## References

- Lublin, D. M., and J. P. Atkinson. 1989. Decay-accelerating factor: biochemistry, molecular biology, and function. *Annu. Rev. Immunol.* 7:35.
- Nicholson-Weller, A., and C. E. Wang. 1994. Structure and function of decay accelerating factor CD55. *J. Lab. Clin. Med.* 123:485.
- Nicholson-Weller, A., J. P. March, C. E. Rosen, D. B. Spicer, and K. F. Austen. 1985. Surface membrane expression by human blood leucocytes and platelets of decay accelerating factor, a regulatory protein of the complement system. *Blood* 65:1237.
- Zimmerman, A., H. Gerber, V. Nussenzweig, and H. Isliker. 1990. Decay-accelerating factor in the cardiomyocytes of normal individuals and patients with myocardial infarction. *Virchows Arch. A Pathol. Pathol. Anat.* 417:299.
- Quigg, R. J., A. Nicholson-Weller, A. V. Cybulsky, J. Badalamenti, and D. J. Salant. 1989. Decay accelerating factor regulates complement activation on glomerular epithelial cells. *J. Immunol.* 142:877.
- Koretz, K., S. Bruderlein, C. Henne, and P. Moller. 1992. Decay-accelerating factor (DAF, CD55) in normal colorectal mucosa, adenomas and carcinomas. *Br. J. Cancer.* 66:810.
- Coyne, K. E., S. E. Hall, E. S. Thompson, M. A. Arce, T. Kinoshita, T. Fujita, D. J. Anstee, W. Rosse, and D. M. Lublin. 1992. Mapping of epitopes, glycosylation sites, and complement regulatory domains in human decay accelerating factor. *J. Immunol.* 149:2906.
- Moran, P., H. Beasley, A. Gorrell, E. Martin, P. Gibling, H. Fuchs, N. Gillett, L. E. Burton, and I. W. Caras. 1992. Human recombinant soluble decay accelerating factor inhibits complement activation in vitro and in vivo. *J. Immunol.* 149:1736.
- Medof, M. E., T. Kinoshita, and V. Nussenzweig. 1984. Inhibition of complement activation on the surface of cells after incorporation of decay-accelerating factor (DAF) into their membranes. *J. Exp. Med.* 160:1558.
- Hamann, J., B. Vogel, G. M. W. Van Schijndel, and R. A. W. van Lier. 1996. The seven-span transmembrane receptor CD97 has a cellular ligand (CD55, DAF). *J. Exp. Med.* 184:1185.
- Shafren, D. R., D. J. Dorahy, R. A. Ingham, G. F. Burns, and R. D. Barry. 1997. Coxsackievirus A21 binds to decay-accelerating factor but requires intercellular adhesion molecule-1 for cell entry. *J. Virol.* 71:4736.
- Nowicki, B., A. Hart, K. E. Coyne, D. M. Lublin, and S. Nowicki. 1993. Short consensus repeat-3 domain of recombinant decay-accelerating factor is recognized by *Escherichia coli* recombinant Dr adhesion in a model of a cell-cell interaction. *J. Exp. Med.* 178:2115.
- Shafren, D. R., R. C. Bates, M. V. Agrez, R. L. Herd, G. F. Burns, and R. D. Barry. 1995. Coxsackieviruses B1, B3 and B5 use decay-accelerating factor as a receptor for cell attachment. *J. Virol.* 69:3873.
- Bergelson, J. M., J. G. Mohanty, R. L. Crowell, N. F. St. John, D. M. Lublin, and R. W. Finberg. 1995. Coxsackievirus B3 adapted to growth in RD cells binds to decay-accelerating factor (CD55). *J. Virol.* 69:1903.
- Bergelson, J. M., B. M. Chan, K. R. Solomon, J. N. St. John, and R. W. Finberg. 1994. Decay-accelerating factor (CD55), a glycosylphosphatidylinositol-anchored complement regulatory protein, is a receptor for several echoviruses. *Proc. Natl. Acad. Sci. USA* 91:6245.
- Clarkson, N. A., R. Kaufman, D. M. Lublin, T. Ward, P. A. Pipkin, P. D. Minor, D. J. Evans, and J. W. Almond. 1995. Characterisation of the echovirus 7 receptor: domains of CD55 critical for virus binding. *J. Virol.* 69:5497.
- Medof, M. E., E. Walter, J. Rutgers, D. Knowles, and V. Nussenzweig. 1985. Soluble DAF in body fluids. *Complement* 2:53.
- Kinoshita, T., M. E. Medof, R. Silber, and V. Nussenzweig. 1985. Distribution of decay accelerating factor in the peripheral blood of normal individuals and patients with paroxysmal nocturnal hemoglobinuria. *J. Exp. Med.* 162:75.
- Fujita, T., T. Inoue, K. Ogawa, K. Iida, and N. Tamura. 1987. The mechanism of action of decay-accelerating factor (DAF): DAF inhibits the assembly of C3 convertases by dissociating C2a and Bb. *J. Exp. Med.* 167:1221.
- Burns, G. F., T. Triglia, J. A. Werkmeister, C. G. Begley, and A. W. Boyd. 1985. TLISA, A human lineage-specific activation antigen involved in the differentiation of cytotoxic T lymphocytes and anomalous killer cells from their precursors. *J. Exp. Med.* 161:1063.
- Sugita, Y., T. Negoro, T. Matsuda, T. Sakamoto, and M. Tomita. 1986. Improved method for the isolation and preliminary characterisation of human DAF (decay-accelerating factor). *J. Biochem.* 100:143.
- Ward, T., P. A. Pipkin, N. A. Clarkson, D. M. Stone, P. D. Minor, and J. W. Almond. 1994. Decay accelerating factor CD55 is identified as the receptor for echovirus 7 using CELICS, a rapid immuno-focal cloning method. *EMBO J.* 13:5070.
- Takeda, A., C. U. Tuazon, and F. A. Ennis. 1988. Antibody-enhanced infection of HIV via Fc receptor-mediated entry. *Science* 242:580.
- Littau, R., I. Kurane, and F. A. Ennis. 1990. Human IgG Fc receptor II mediates antibody-dependent enhancement of dengue virus infection. *J. Immunol.* 144:3183.
- Mason, P. W., B. Baxt, F. Brown, J. Harber, A. Murdin, and E. Wimmer. 1993. Antibody-complexed Foot and Mouth Disease Virus, but not Poliovirus, can infect normally insusceptible cells via the Fc receptor. *Virology* 192:568.
- Faull, R. J., J. Wang, D. I. Leavesely, W. Puzon, G. R. Russ, D. Vestweber, and Y. Takada. 1996. A novel activating anti- $\beta$ 1 integrin monoclonal antibody binds to the cysteine-rich repeats in the  $\beta$ 1 chain. *J. Biol. Chem.* 271:25099.